Analysis of strained surface layers of ZnO single crystals after irradiation with intense femtosecond laser pulses

Andreas Schneider,[1,a)] Daniel Wolverson,[2] Kathrin Sebald,[1] Chris Hodges,[3] Martin Kuball,[3] and Tobias Voss[1]
[1]*Semiconductor Optics, Institute of Solid State Physics, University of Bremen, D-28359 Bremen, Germany*
[2]*Nanoscience Group, Department of Physics, University of Bath, BA2 7AY Bath, United Kingdom*
[3]*Center for Device Thermography and Reliability (CDTR), H. H. Wills Physics Laboratory, University of Bristol, Tyndall Avenue, Bristol BS8 1TL, United Kingdom*

(Received 25 April 2013; accepted 13 May 2013; published online 28 May 2013)

Structural modifications of ZnO single crystals that were created by the irradiation with femtosecond laser pulses at fluences far above the ablation threshold were investigated with micro-Raman spectroscopy. After light-matter interaction on the femtosecond time scale, rapid cooling and the pronounced thermal expansion anisotropy of ZnO are likely to cause residual strains of up to 1.8% and also result in the formation of surface cracks. This process relaxes the strain only partially and a strained surface layer remains. Our findings demonstrate the significant role of thermoelastic effects for the irradiation of solids with intense femtosecond laser pulses. © *2013 AIP Publishing LLC*. [http://dx.doi.org/10.1063/1.4807923]

Ultrashort laser pulses are often favorable for material processing due to their high precision in material removal and small ambient damage compared to techniques using longer laser pulses.[1,2] They create highly non-equilibrium conditions at the surface of the processed materials, so that nonthermal mechanisms play a pronounced role for the dynamics of the excited material states.[3,4] Surface instabilities result in the formation of regular patterns on the nano- or micrometer scale under specific circumstances.[5] For silicon, femtosecond (fs) laser pulses have been used to create arrays of micro-cones that drastically increase the surface-to-volume ratio and thereby allow one to increase the above-bandgap light absorption of silicon devices.[6,7] Surface ripples are the most prominently observed surface patterns after structuring of numerous solids with fs laser pulses.[8] ZnO is a prominent member of this material class, and ripple formation has been thoroughly studied for ZnO single crystalline materials.[9–11] In addition, optical hyperdoping of silicon using fs laser pulses has recently attracted considerable attention as it allows for the fabrication of functional layers that can be used in silicon-based IR photodetectors or black silicon solar cells.[12,13] Recently, the transfer of this technique to the ZnO material system has been demonstrated,[14] which can potentially pave the way for a new doping strategy of binary oxide semiconductors in general.

However, little is known about the residual strain state of the materials after the interaction with fs-laser pulses, which is important if surfaces with tailored functionalities are to be created. In ablation experiments on InP, Bonse *et al.*[15] found that surface regions could remain under compressive as well as under tensile strain. These strain regions extend microns into the material as reported by Borowiec *et al.*[16] Compressed regions were also found in silicon.[17] This compression was explained by the recoil pressure due to the ablation.

In this letter, we analyze fs laser pulse induced surface structures of ZnO single crystals in regard to residual strain in the surface layer. We look at surface structures induced by laser pulses with peak fluences far above the ablation threshold where no ripples form. Analyzing ZnO with respect to possible residual strain is especially interesting because of its increasing technological use for optoelectronic devices.[18] The performance of such devices may depend crucially on the quality of laser processed ZnO. So far, there have been no studies for ZnO concerning the resulting strain state due to ultrashort pulse processing.

For our investigations, we used hydrothermally grown ZnO (Crystec GmbH, thickness 330 μm) with an epi-polished c-plane surface. The samples were placed in a vacuum chamber mounted on a motorized xy translation stage. During the experiments, the pressure was kept at 2×10^{-2} mbar. A regenerative titanium sapphire amplifier system served as ultrashort laser pulse source. The linearly polarized laser pulses had a duration of 100 fs at a central wavelength of 795 nm and were focused perpendicular to the sample surface. The peak fluence of the Gaussian beam at the sample surface was (9.0 ± 0.7) J/cm^2, far above the single pulse ablation threshold of ZnO of (0.5 ± 0.1) J/cm^2. This value was determined for our samples in a separate ablation experiment according to the method of Liu.[19] An electronic shutter was used to control the number of incident laser pulses on the surface.

When these laser pulses hit the surface material, light absorption processes will transfer enough energy into the ZnO crystal to ablate a certain amount of material. This ablation process will form a crater on the surface. We analyzed the surface morphology after 1, 2, and 10 laser pulses using a scanning electron microscope. Furthermore, we investigated the craters with a Raman microscope (Renishaw RM 2000 NUV) using a continuous wave HeCd laser emitting at a wavelength of 325 nm. Raman spectra were recorded across the fs pulse induced surface modifications. The microscope laser spot size was 2 μm in diameter. The spectrometer could resolve the shifts down to 0.2 cm^{-1}. Under the given excitation conditions, a sample depth $1/\alpha$ of 60-70 nm could be probed (linear absorption coefficient $\alpha \approx 1.6 \times 10^5$ cm^{-1}).[20]

a)Electronic mail: schneider@ifp.uni-bremen.de.

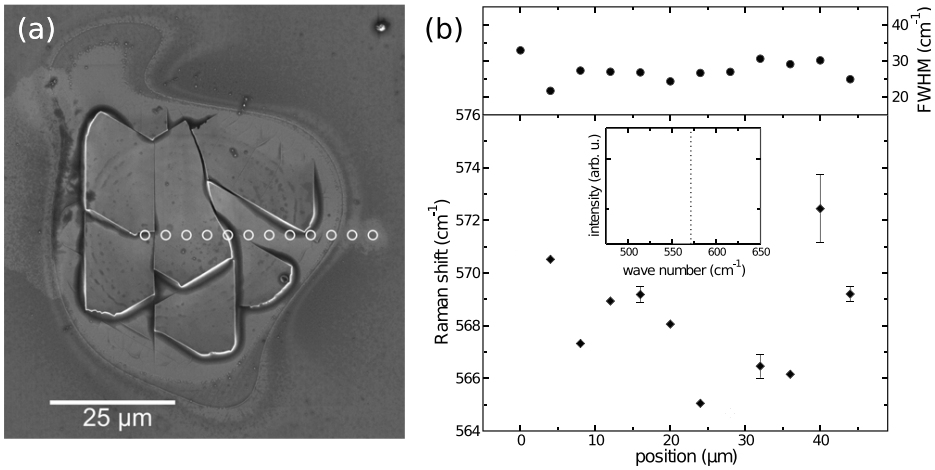

FIG. 1. (a) Scanning electron micrograph showing the ZnO surface after the modification by a single ultrashort laser pulse with a peak fluence of 9 J/cm^2. The white circles illustrate the points where Raman spectra were recorded. (b) Line widths (top) and center positions (bottom) of the A_1(LO) phonon modes as obtained from the Raman scattered signal at the positions marked in (a). The inset shows Raman spectra measured at the position marked in red and blue.

All Raman spectra were recorded in backscattering geometry and at room temperature.

Fig. 1(a) shows the surface modifications caused by a single femtosecond pulse (peak fluence 9 J/cm^2). In contrast to our ablation experiments with smaller laser fluences (data not shown), the crater structure is not the most distinctive feature. Instead, the surface morphology is dominated by surface cracks that form lamellae detached from the underlaying material. This delamination is most pronounced in the center of the crater. Here, the lamella is up to 700 nm thick. Outside the central region, the lamellae become thinner, and the delamination is smaller. Near the crater rim, only cracking of the surface is apparent with no visible delamination. Since the phonon frequency is sensitive to lattice deformations, phonon Raman scattering can be used to analyze the strain state of the crystal. ZnO has a wurtzite structure (C_{6v} symmetry), and group theory predicts phonon modes with the symmetry: A_1, B_1, E_1, and E_2.[21] From those modes that are Raman active, selection rules allow one to study the E_2^{low}, E_2^{high} and A_1(LO) mode in z(xx)-z backscattering geometry. The circles in Fig. 1(a) mark the positions where Raman spectra were recorded. The z axis is chosen to lie parallel to the hexagonal c-axis. Due to the resonant excitation, we were only able to analyze spectra corresponding to the A_1(LO) phonon mode. Fig. 1(b) shows the Raman shift of this mode for the marked areas in Fig. 1(a) across the modifications. The inset of Fig. 1(b) displays Raman spectra for two representative positions. The frequency of the mode was obtained by fitting a Lorentzian profile to the measured Raman data. Within the mapped area on the sample, the mode shifts in total from smallest to largest frequency by as much as 8 cm^{-1}.

The results point to a modified strain state of the near surface material causing the observed behavior, since we can exclude several other mechanisms for this mode shift. First, we can rule out that the resonant excitation of ZnO during the Raman measurements leads to a local heating of the sample resulting in a broadening and a shift of the A_1(LO) to a smaller wave number. The spectra recorded at different excitation intensities did not reveal any significant shift or broadening of the mode. Second, we observe no upward shift and broadening of the mode. Polar phonons, as the A_1 mode, are in general sensitive to interactions with free carriers. When the plasmon frequency approaches the LO phonon frequency, a strong coupling occurs and LO-plasmon-coupled modes are observed.[22] Due to the large plasmon damping, only the upper branch was observed for ZnO.[23] For increasing carrier concentrations, the observed mode is expected to broaden and its Raman shift is expected to increase.[24] Therefore, a change of free carrier concentrations is not the reason for the shifts presented in Fig. 1(b). Third, phonon confinement in ZnO nano-crystals would downshift and broaden Raman lines.[25] However, we do not observe a broadening of the downward shifted modes.

The different strain state is caused by uniaxial stress acting on the sample surface. It has its origin in the heating of the sample and the ablation process due to the laser-matter interaction. To estimate the residual strain left in the sample after the laser treatment, we assume that the in-plane strain is isotropic, $\epsilon_{xx} = \epsilon_{yy}$. Because of the small accessible probe depth, we assume further that the layer is uniformly strained. In this case, the out-of-plane component of the strain tensor ϵ_{zz} is connected to the in-plane component ϵ_{xx} by $\epsilon_{zz} = -\frac{C_{13}}{C_{33}}(\epsilon_{xx} + \epsilon_{yy})$.[26,27] C_{ij} are the elastic constants of ZnO with $C_{13} = 104.8$ GPa and $C_{33} = 206.9$ GPa.[28] The strain of the crystal results in a shift of the zone center optical phonon frequencies. The magnitude of that frequency shift $\Delta\omega$ in the linear strain approximation is given by[29]

$$\Delta\omega = a(\epsilon_{xx} + \epsilon_{yy}) + b\epsilon_{zz}\,,\psi \tag{1}$$

where a and b are the deformation potential constants. Under uniaxial strain, $a = -577\,\mathrm{cm}^{-1}$ and $b = -599\,\mathrm{cm}^{-1}$ are reported as values for the A_1(LO) mode of ZnO.[30] With the above mentioned assumptions, Eq. (1) can be simplified to

$$\Delta\omega = \left(-a\frac{C_{33}}{C_{13}} + b\right)\epsilon_{zz}\,.\psi \tag{2}$$

Equation (2) was used to calculate the residual strain in the sample. To obtain the frequency shift, the unstrained A_1(LO) phonon frequency of 572.7 cm^{-1} was measured at an unaffected ZnO surface in the proximity of the investigated craters.

Fig. 2 displays the calculated in-plane ϵ_{xx} and out-of-plane strain ϵ_{zz} of a sample region treated by a single (a)

and two (b) laser pulses at 9 J/cm^2. In both cases, the surface layer is compressively strained along the c-axis and as a consequence is under tensile strain in the perpendicular direction. Because of the elastic constants of ZnO, the absolute value of the in-plane and out-of-plane components are almost identical. The measured values are subject to an error of 38%, calculated using the reported uncertainties of the involved constants taken from literature.[28,30]

Several forces lead to a stressed surface layer during laser ablation. Studies have shown that, even for ultrashort laser pulses, a transient liquid layer is formed below the ablation zone.[31] The spatial intensity variation of the laser pulse results in a temperature gradient across the liquid layer causing thermocapillary forces. Furthermore, the ablation itself brings about a large recoil pressure acting on the substrate.[32] Beside this recoil pressure and thermocapillary forces acting on the thin transient molten layer, another source of stress occurs once the molten layer has resolidified. The pronounced thermal expansion anisotropy of solid ZnO (Ref. 33) generates thermal stresses when temperature changes occur inside the material. As the thermal expansion coefficient parallel to the crystal c-axis is smaller than that normal to the axis, the crystal will be strained compressively along its c-axis during the rapid cooling, matching our observations. When the fracture stress is reached, surface cracks will form.

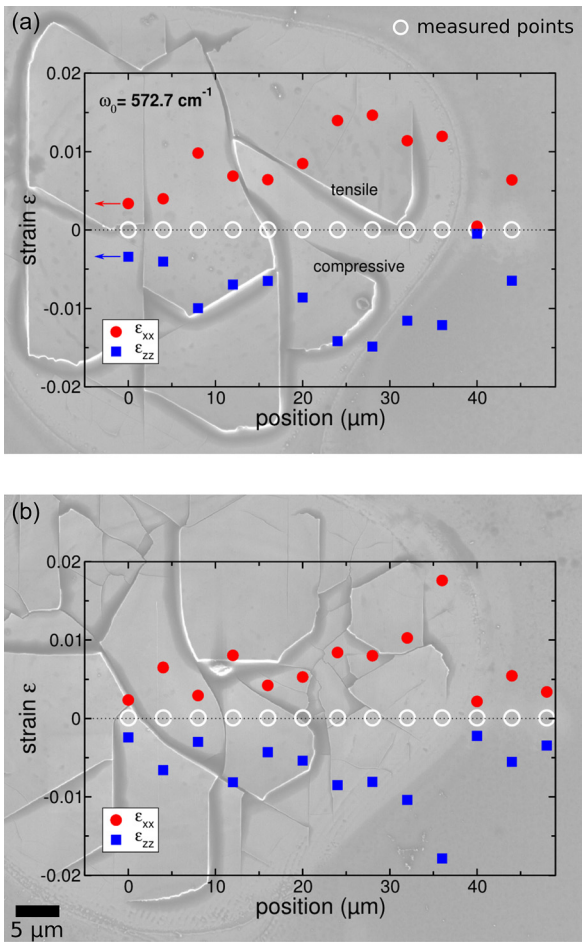

FIG. 2. In-plane ϵ_{xx} and out-of-plane components ϵ_{zz} of the strain tensor calculated from the Raman data at the positions of the measurements on the samples. Shown is the morphology and the strain after (a) one ultrashort pulse and (b) two ultrashort pulses with a peak fluence of 9 J/cm^2.

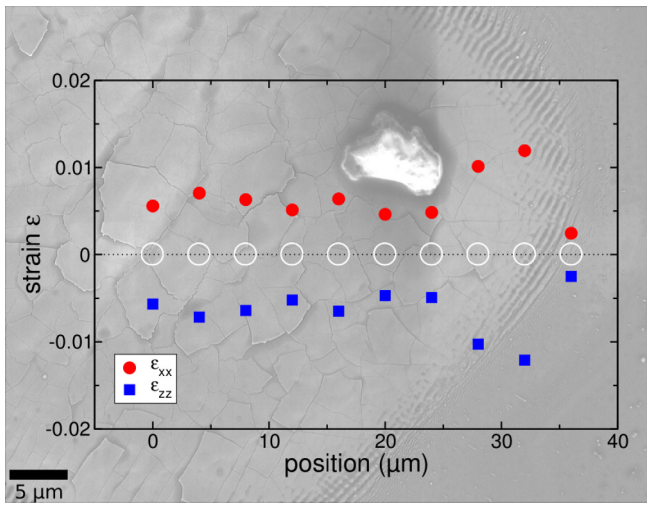

FIG. 3. Strain values calculated from Raman data at different spots across a crater created by 10 ultrashort laser pulses.

Our results clearly show that strain relaxation via cracking does not compensate the strain completely and surface regions remain strained. The variation of the strain along the surface, shown in Fig. 2, might reflect the degree of relaxation. Strain as large as 1.8% can be found. Although no clear trend can be seen in the experimentally determined strain of the central region of the crater, an increase of the strain is observed near the crater rim in each measurement (Figs. 2 and 3). In this region, no or less cracking occurred and therefore less relaxation took place. By applying a second laser pulse, the observed maximal strain value is 20% larger than what is observed after one pulse. This suggests strain accumulation. The number of cracks is larger after two pulses because the thermal stress induced by the second pulse breaks up the existing lamellae. The accumulation of strain due to multiple pulses is likely to be obscured by the relaxation via cracking. This can be seen in Fig. 3, which shows strain values and the surface morphology after 10 laser pulses. The average size of the crack tile is now only 7.5% of the average size after two laser pulses, and the thickness of the lamellae is less than 100 nm. This is accompanied by a smaller variation of the observed strain. Excluding the crater rim, the measured strain values fluctuate on average by 51% at the two pulse crater but only 19% at the 10 pulse crater.

There are few comparable studies in the literature. For InP, regions with compressive as well as tensile stress were found near the surface of craters created by ultrashort pulse ablation.[15] In comparison to our experiments, the peak laser fluence used to create a crater in this experiment was only 1.8 J/cm^2. However, the ablation threshold of ZnO is 2.2 times larger than the threshold of InP for the given laser parameters, which reduces the difference in the excess energy input to a factor of 2.3. Hence, there are comparable regions near the crater rim. Bonse *et al.*[15] found the largest strain value near the crater rim, matching our observation for the crater structured by two laser pulses (Fig. 2(b)). In addition, they observed a broadening of the LO peak for the downward shifted modes, which has been attributed to the presence of nanocrystalline InP. In our experiment, we neither found signatures of polycrystalline material near the surface

inside the crater nor did we detect amorphous ZnO outside the crater. This is due to the fact that ZnO has a large bond ionicity and therefore preferentially solidifies in a crystalline phase. Furthermore, InP does not exhibit a thermal expansion anisotropy, and therefore, only spatial temperature gradients could contribute to thermal stress acting on the solid during the cooling. Simultaneously, no large scale cracks were observed.[16] This indicates that residual strain due to ultrashort laser pulses might have a different, material dependent origin and relies crucially on the thermal and elastic properties of the solid.

In summary, we have analyzed residual strain in ZnO caused by the application of ultrashort laser pulses with pulse energies far above the threshold for ablation. Rapid cooling in combination with the thermal expansion anisotropy results in strain of up to 1.8% near the surface. The maximal residual strain found after two laser pulses was 20% larger than the strain caused by a single laser pulse of 9 J/cm^2. Extensive surface cracking was observed as result of stress exceeding the fracture limit of ZnO. These findings confirm that strain is a significant factor to understand accumulation effects that change, for instance, the ablation threshold and typically occur when applying multiple laser pulses on a single spot. These accumulation effects are important for laser processing applications, as they need to be taken into account in order to realize precise material processing.[34,35] In addition, our findings show that thermoelastic effects due to heating by ultrashort laser pulses play a significant role in the interaction with ZnO.

We thank the DAAD (scholarship D/11/42417) and the BFK of the University of Bremen (Project ZFK 01/132/08) for their financial support of this work. Furthermore, we thank Professor Dr. Jürgen Gutowski for a valuable discussion and critical reading of the manuscript.

[1]H. Varel, D. Ashkenasi, A. Rosenfeld, M. Wähmer, and E. E. B. Campbell, Appl. Phys. A: Mater. Sci. Process. **65**, 367 (1997).
[2]X. Liu, D. Du, and G. Mourou, IEEE J. Quantum Electron. **33**, 1706 (1997).
[3]T. Shih, E. Mazur, J.-P. Richters, J. Gutowski, and T. Voss, J. Appl. Phys. **109**, 043504 (2011).
[4]T. Shih, M. Winkler, T. Voss, and E. Mazur, Appl. Phys. A **96**, 363 (2009).
[5]N. M. Ghoniem and D. Walgraef, *Instabilities and Self-Organization in Materials: Applications in Materials Design and Nanotechnology* (Oxford University Press, Oxford, 2008).
[6]T.-H. Her, R. J. Finlay, C. Wu, S. Deliwala, and E. Mazur, Appl. Phys. Lett. **73**, 1673 (1998).
[7]C. Wu, C. H. Crouch, L. Zhao, J. E. Carey, R. Younkin, J. A. Levinson, E. Mazur, R. M. Farrell, P. Gothoskar, and A. Karger, Appl. Phys. Lett. **78**, 1850 (2001).
[8]J. Bonse, J. Krüger, S. Höhm, and A. Rosenfeld, J. Laser Appl. **24**, 042006 (2012).
[9]M. Huang, F. L. Zhao, T. Q. Jia, Y. Cheng, N. S. Xu, and Z. Z. Xu, Nanotechnology **18**, 505301 (2007).
[10]X. Guo, R. Li, Y. Hang, Z. Xu, B. Yu, H. Ma, B. Lu, and X. Sun, Mater. Lett. **62**, 1769 (2008).
[11]D. Dufft, A. Rosenfeld, S. K. Das, R. Grunwald, and J. Bonse, J. Appl. Phys. **105**, 034908 (2009).
[12]Z. Huang, J. E. Carey, M. Liu, X. Guo, E. Mazur, and J. C. Campbell, Appl. Phys. Lett. **89**, 033506 (2006).
[13]T. Sarnet, J. E. Carey, and E. Mazur, AIP Conf. Proc. **1464**, 219 (2012).
[14]A. Schneider, A. Dev, K. Sebald, K. Frank, A. Rosenauer, and T. Voss, J. Appl. Phys. **113**, 143512 (2013).
[15]J. Bonse, J. Wrobel, K.-W. Brzezinka, N. Esser, and W. Kautek, Appl. Surf. Sci. **202**, 272 (2002).
[16]A. Borowiec, D. M. Bruce, D. T. Cassidy, and H. K. Haugen, Appl. Phys. Lett. **83**, 225 (2003).
[17]M. J. Smith, Y.-T. Lin, M.-J. Sher, M. T. Winkler, E. Mazur, and S. Gradeçak, J. Appl. Phys. **110**, 053524 (2011).
[18]C. F. Klingshirn, A. Waag, A. Hoffmann, and J. Geurts, *Zinc Oxide: From Fundamental Properties Towards Novel Applications* (Springer, Berlin, Heidelberg, 2010).
[19]J. M. Liu, Opt. Lett. **7**, 196 (1982).
[20]H. Morkoç and U. Özgür, *Zinc Oxide: Fundamentals, Materials and Device Technology* (John Wiley & Sons, Weinheim, 2008).
[21]R. Loudon, Adv. Phys. **13**, 423 (1964).
[22]G. Abstreiter, M. Cardona, and A. Pinczuk, in *Light Scattering in Solids IV*, edited by M. Cardona and G. Güntherodt (Springer, Berlin, Heidelberg, 1984), Vol. 54, pp. 5–150.
[23]A.-J. Cheng, Y. Tzeng, H. Xu, S. Alur, Y. Wang, M. Park, T.-h. Wu, C. Shannon, D.-J. Kim, and D. Wang, J. Appl. Phys. **105**, 073104 (2009).
[24]B. H. Bairamov, A. Heinrich, G. Irmer, V. V. Toporov, and E. Ziegler, Phys. Status Solidi B **119**, 227 (1983).
[25]M. Rajalakshmi, A. K. Arora, B. S. Bendre, and S. Mahamuni, J. Appl. Phys. **87**, 2445 (2000).
[26]V. Darakchieva, T. Paskova, M. Schubert, H. Arwin, P. P. Paskov, B. Monemar, D. Hommel, M. Heuken, J. Off, F. Scholz, B. A. Haskell, P. T. Fini, J. S. Speck, and S. Nakamura, Phys. Rev. B **75**, 195217 (2007).
[27]V. Y. Davydov, N. S. Averkiev, I. N. Goncharuk, D. K. Nelson, I. P. Nikitina, A. S. Polkovnikov, A. N. Smirnov, M. A. Jacobson, and O. K. Semchinova, J. Appl. Phys. **82**, 5097 (1997).
[28]I. Shein, V. Kiĭko, Y. Makurin, M. Gorbunova, and A. Ivanovskiĭ, Phys. Solid State **49**, 1067 (2007).
[29]R. J. Briggs and A. K. Ramdas, Phys. Rev. B **13**, 5518 (1976).
[30]G. Callsen, J. S. Reparaz, M. R. Wagner, R. Kirste, C. Nenstiel, A. Hoffmann, and M. R. Phillips, Appl. Phys. Lett. **98**, 061906 (2011).
[31]A. Ben-Yakar, A. Harkin, J. Ashmore, R. L. Byer, and H. A. Stone, J. Phys. D: Appl. Phys. **40**, 1447 (2007).
[32]D. Bäuerle, *Laser Processing and Chemistry*, 4th ed. (Springer, Berlin, Heidelberg, 2011).
[33]H. Iwanaga, A. Kunishige, and S. Takeuchi, J. Mater. Sci. **35**, 2451 (2000).
[34]Y. Jee, M. F. Becker, and R. M. Walser, J. Opt. Soc. Am. B **5**, 648 (1988).
[35]D. Ashkenasi, M. Lorenz, R. Stoian, and A. Rosenfeld, Appl. Surf. Sci. **150**, 101 (1999).